International Journal of Scientific Research in Physics and Applied Sciences
Vol.**12**, Issue.**2**, pp.**26-33**, April **2024**
E-ISSN: 2348-3423
Available online at: www.isroset.org

Research Article

Characterization and Wet Chemical Synthesis of Magnesium Tartrate Nano Particles

U.M. Lathiya[1*], M.J. Joshi[2], P.M. Vyas[3]

[1,2]Crystal Growth Laboratory, Department of Physics, Saurashtra University, Rajkot – 360005, Gujarat, India
[3]Physics Department, Kamani Science College, Amreli - 365601, Gujarat, India

**Corresponding Author: urvi.tarpara@gmail.com*

Received: 26/Feb/2024; **Accepted**: 29/Mar/2024; **Published**: 30/Apr/2024

Abstract— Magnesium tartrate is having application in purgative and food supplement formulations. Magnesium tartrate nanoparticles are obtained by employing the wet chemical method. Aqueous solutions of $MgCl_2$, tartaric acid, and sodium metasilicate (SMS) solutions are added together in the presence of Triton X-100 surfactant in the desired manner. The SMS helps in the formation of magnesium tartrate products. The powder XRD analysis indicates the orthorhombic nature of the magnesium tartrate nano-particles with the 40.35 nm average crystallite size from Scherrer's method and 10.90 nm from the W-H (Williamson-Hall) method. The particle size and the morphology of nano-particles are studied by using TEM. The FTIR spectrum confirms the functional groups, viz., C-H, O-H, and C=O in the sample. TGA indicates the thermal stability up to 213^o C and then decomposition occurs via different stages. The dielectric analysis is reported on the pellet form of the sample within the range of frequency from 10 Hz to 10 MHz and temperature from 303K to 363K. The variation in both dielectric constant and dielectric loss along with the frequency of applied field suggests decreasing nature in the values as the frequency increases. However, the reverse trend is displayed for the A.C. conductivity with increasing frequency. Various parameters are evaluated from Jonscher's power law and the CBH (Correlated Barrier Hopping) model for A.C. conductivity is suggested from the analysis.

Keywords— Magnesium tartrate nanoparticles, powder XRD, TEM, FTIR, TGA, Dielectric Properties.

1. Introduction

Tartaric acid and metal salts are the precursors for the formation of metallic tartrate compounds, however, the reaction is not straightforward, and often the gel medium is used for the growth of crystals [1],[2]. The role of sodium metasilicate in the synthesis of crystalline and nanoparticles of metal tartrate compounds is well explained by Vyas et al. [2] and Tarpara et al [3]. Earlier in our lab, we used the sodium metasilicate (SMS) gel medium to generate various metal tartrate crystals [4],[5],[6],[7],[8]. For last more than two decades and nanoparticles of various metal tartrates have been synthesized and characterized recently the nano particles of calcium tartrate and strontium tartrates are also reported [3],[9]. There are very scanty reports available on magnesium tartrate, for example, the chemical and structural diversity in chiral magnesium tartrate [10], the gross morphology of magnesium (D, L) tartrate [11], the use of magnesium tartrate in the colonic purgative formulation [12], in the non-critical phase matching using magnesium tartrate at 0.92 μm wavelength [13] as a precursor to synthesize MgO nanoparticles by sol-gel method [14]. Magnesium is the fourth most common cation in the human body and participates in more than 1000 enzymatic reactions, the magnesium tartrate is used in formulation to increase the uptake of magnesium in mammals [15], Magnesium tartrate also finds application in the growth inhibition of urinary type calcium oxalate crystals [16],[17]. There are only a few reports available on the growth of magnesium tartrate crystals, Viz., by hydrothermal method [10] and gel growth [18]. The recovery of magnesium tartrate is reported by Ghara et al [19] in the recovery of potassium salts from the sea bittern.

The novelty of the present work is that, by careful literature survey, one finds no significant work reported on magnesium tartrate nanoparticles synthesis and characterization. This has motivated me to synthesize magnesium tartrate nanoparticles by cost-effective wet chemical surfactant mediated approach at the ambient temperatures and characterized by Powder XRD and TEM to confirm the nanostructured nature, FTIR for the knowledge of the functional groups, TG – DTA for the thermal stability study, dielectric study for the change in various dielectric and electrical properties with the frequency of the applied field.

2. Experimental Technique

The nano-particles of magnesium tartrate were achieved from a wet chemical surfactant mediated approach. The method is discussed elsewhere in detail [3]. Aqueous solutions of 2M $MgCl_2$, 1 M d-tartaric acid ($H_2C_4H_4O_6$), and sodium metasilicate (SMS) of specific gravity 1.05 were added under constant stirring with Triton X-100 (surfactant) in such a way that proper water/ surfactant ratio and mixture pH remains between 4.0 to 5.0. AR grade chemicals were used. The SMS solution helped in the chemical process to form the product without participating in the reaction, which is elaborately explained elsewhere by the present workers [2],[3].

The white color precipitates were filtered followed by a wash using de-ionized water and air-dried. The chemical reaction occurring is as follows without indicating the role of SMS:

$$MgCl_2 + H_2C_4H_4O_6 \rightarrow MgC_4H_4O_6 + 2HCl$$

PHILIPS X'PERT MPD set up with Cu Kα radiation used for powder XRD study and data in .udf format were analyzed by computer software Powder X. The TEM images were captured on Philips Tecnai 20 (SAIF, IIT Bombay) by dispersing samples into acetone. Nicolet 6700 was employed for recording FTIR spectrum in the range from 400 cm^{-1} to 4000 cm^{-1}. METTLER TOLEDO TGA/SDTA 851 setup was used to analyze the sample in the atmosphere of nitrogen with a heating rate of 25 °C/min from RT (room temperature) to 700°C. For the dielectric study, the palletized sample was used for the measurements using the HIOKI 3532 LCR HITERSTER meter at temperatures from 303K to 373K within the range of frequency from 10 Hz to 10 MHz.

3. Results and Discussion

3.1 Powder XRD

Figure 1 displays the powder XRD pattern of magnesium tartrate nano-particles sample. The peak around 35° shows maximum and broadening of maximum peak having a hkl parameters [332]. From the data analysis the unit cell dimensions were obtained as: a = 9.19 Å, b = 11.18 Å, c = 7.96 Å and α = β = γ = 90^0. These unit cells are in good agreement with previously reported by Dave et al. [18] which are, a = 9.18 Å, b = 11.20 Å, c = 7.95 Å and α = β = γ = 90^0 .

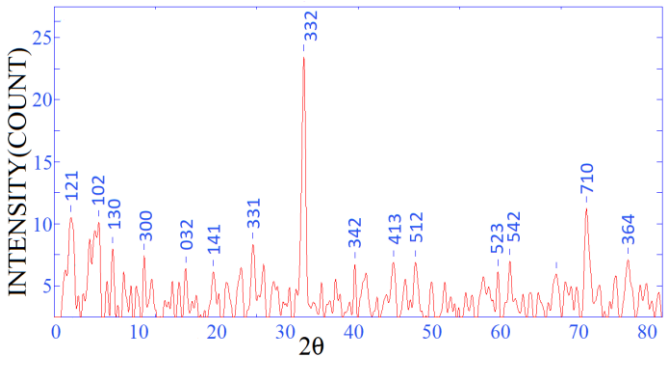

Figure 1. Powder XRD pattern of magnesium tartrate nanocrystalline particles

The average crystallite size was evaluated by using the FWHM of maximum peak with two different methods, i.e., Scherrer's as well as Williamson and Hall's (W-H) methods, and found as 40.35 nm and 10.90 nm, respectively. The strain present in the crystallites was estimated from the W-H analysis method as 0.0126. The difference between the values of average particle size obtained from the Scherrer's formula and Williamson-Hall method is due to their different approaches. The Scherrer's formula takes the Gaussian fit approach to the peaks in the XRD patterns, whereas the Williamson-Hall method considers the limited crystallite size and crystallographic distortion, i.e., the strain, leading to the Lorentzian intensity distribution [20],[21].

3.2 TEM

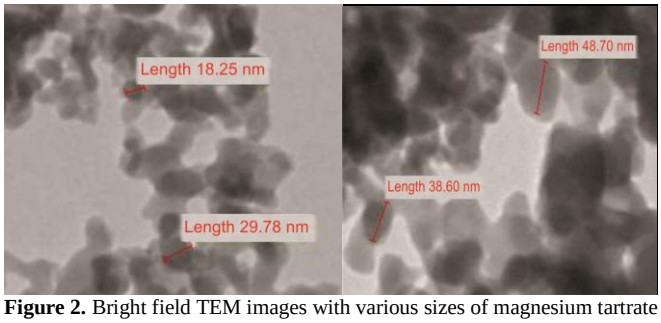

Figure 2. Bright field TEM images with various sizes of magnesium tartrate nanoparticles

The TEM images reveal details of size, shape, and the type of morphology of nano-systems. Before putting the sample in sample holder of TEM powdered sample of magnesium tartrate nano particles were dispersed in acetone. Figure 2 displays the TEM images. The majority of particles are within 15 nm to 50 nm in the observed frame having a minimum size of 18.25 nm and a maximum size of 48.70 nm. Although the nano-particles exhibit an aggregated nature, the overall distribution indicated a reasonably small range of diameter variation with a nearly spherical nature.

3.3 FTIR

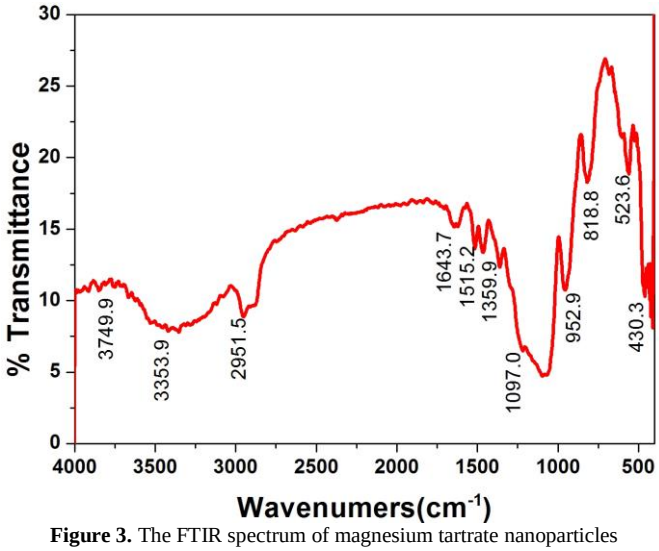

Figure 3. The FTIR spectrum of magnesium tartrate nanoparticles

Infrared spectroscopy reveals information about molecular vibrations that cause a change in the dipole moment of molecules. It offers a fingerprint of the chemical bonds present within materials. Figure 3 exhibits the FTIR spectrum of magnesium tartrate nanoparticles. Table 1 exhibit the assignment and bond present in magnesium tartrate nanoparticles. The absorption band at 3749.9 cm^{-1} is attributed to the O–H asymmetric stretching mode, while the band observed at 3353.9 cm^{-1} is because of O–H symmetric stretching mode. The C–H stretching vibration mode is observed at 2951.5 cm^{-1}. The bands observed at 1643.7 cm^{-1} and 1515.2 cm^{-1} are due to C=O stretching mode. The band observed at 1359.9 cm^{-1} is due to O-H in plane bending and the C–O stretching mode is observed at 1097.0 cm^{-1}. Moreover, the O–H out of plane bending mode is revealed at 952.9 cm^{-1} and 818.8 cm^{-1}. The absorptions at 523.6 cm^{-1} and 430.3 cm^{-1} are due to metal-oxygen vibrations. Comparing the present FTIR spectrum of magnesium tartrate nanoparticles with the reported FTIR spectrum of magnesium tartrate crystal by Dave et al [18], it was noticed that certain absorption peaks shift either higher wavenumbers or lower wavenumbers in nanostructured samples. For instance, in a nanostructured sample the O–H stretching mode absorption is getting shifted to higher values of wavenumbers and for the C–O stretching and bending vibration modes the shifting is taking place towards lower wavenumbers. The red and blue shifts occurring in the spectrum of nano-structured sample FTIR spectrum in comparison to that of the bulk is mainly having a larger surface to volume ratio, surface interaction, interfacial effects, the change taking place in the restoring force created by the surface polarization charge, and dangling bonds present in nanostructured material as discussed earlier [3],[22].

Table 1: FTIR assignment for magnesium tartrate nanoparticles

Wavenumber cm^{-1}	Assignment
3749.9	O–H asymmetric stretching mode
3353.9	O–H symmetric stretching mode
2951.5	C–H stretching
1643.7	C=O stretching mode
1515.2	
1359.9	O-H in-plane bending
1097.0	C–O stretching mode
952.9	O–H out of plane bending mode
818.8	
523.6	metal-oxygen vibrations
430.3	

The expression shows the relation between the absorption frequency in the FTIR spectrum for particular di-atomic stretching vibration and from that, the value of the force constant is evaluated as [23]

$$\nu = 1303\sqrt{F\left(\frac{1}{M_1}+\frac{1}{M_2}\right)} \quad \text{--------- (1)}$$

Where, 1303 = $\sqrt{N_A \times 10^5}$ /2πc, N_A is the Avogadro's number (6.0225 $\times 10^{23} mol^{-1}$) and c = Speed of light = 3×10^{10} cm/s. By taking up a simple model for di-atomic stretching vibration [24], the value of force constant obtained for O-H stretching vibrations using equation (1) at 3749.9 cm^{-1} is 753 N/m for magnesium tartrate nano-particles. Whereas for the bulk magnesium tartrate, the value of force constant evaluated for the same O – H stretching vibrations occurring at 3452 cm^{-1} is equal to 638 N/m [18]. The larger force constant value of O-H vibration for the nanomaterial is attributed to the larger ratio of surface to volume as well as the larger surface energy for the nanostructured sample.

3.4 TGA/DTA

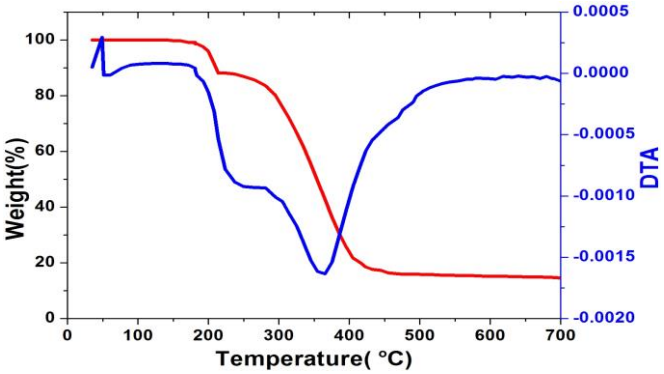

Figure 4. TG-DTA of Magnesium Tartrate nanoparticles

Figure 4 displays the TG- DTA traces of magnesium tartrate nanoparticles. The magnesium nano particles were heated at a rate of 25°C/min from room temperature to 700°C in nitrogen atmosphere to avoid any oxidation during heating of the sample. Initially, on heating, the synthesized sample gets converted to anhydrous form at 213°C and then decomposes precipitously from 213°C to a brief meta-stable state at 365°C by converting it into magnesium carbonate form. In the final stage the decomposition occurs from 365°C to 415°C, the sample attains magnesium oxide form by slow decomposition.

Table 2: TG-DTA decomposition behavior and product formed during thermal study

Temperature (°C)	Theoretical Weight %	Experimental Weight %	Nature of Reaction	Product Formed	Remark
RoomTemperature	100	100	exothermic	Hydrated sample	
213	88.04	88.16	----	Anhydrous	Removal of moisture
365	43.06	42.80	endothermic	Mg-carbonate	Decomposition of dehydrated sample
415	20.58	20.05	---	Mg-Oxide	Due to decomposition of magnesium carbonate

DTA study shows the minor endothermic reaction observed at 60^o C temperature, which is a result of giving up the water of hydration or moisture. The large endothermic peak observed at 365^oC is due to the decomposition of the sample into carbonate form. Table 2 shows the theoretical and experimental weight percentage of the sample, nature of the reaction, and product formed at different temperatures. From the analysis, the presence of one water molecule was found.

The thermal stability of magnesium tartrate nano-particles is higher than the physiological temperatures and ensures a higher shelf life for storage applications in reference to bio-medical use.

3.5 Dielectric study

The dielectric study is important for getting insight into the polarization behavior, conduction mechanisms, and dielectric relaxation [25]. The dielectric properties are very important in pharmaceutical applications. The important role of the dielectric constant in drug solubility prediction has been discussed by Fakhree et al [26]. Moreover, the roles of metal ions like magnesium in the biological function of many enzymes serve as electron donors or acceptors [27]. The kinetics of charge transfer depends on the dielectric organization of the medium in the enzymatic reactions [28] and magnesium is playing a very important role in several enzymatic reactions. Magnesium tartrate is figured out in application as purgative [12] and food supplement [15] and hence looking at the important role of magnesium and magnesium based compounds, the present authors carried out dielectric studies of magnesium tartrate nano-particles samples.

According to general observation, the dielectric constant varies with the frequency of applied field, the temperature of the sample, orientation, mixture of different compounds, pressure, and molecular structure of the material [29]. In the literature, several reports are available on dielectric studies of various substances at different temperatures and frequencies to understand the conduction mechanism prevailing, for instance, strontium tartrate crystals [30], $CuWO_4$ crystals [31], Ge $S_{0.25}$ $Se_{0.75}$ single crystals [32], gadolinium fumarate crystals [33], L-threonine doped ADP crystals [34], cadmium titanate nanofiber mats [35] and fish scales [36]. Dielectric relaxation and complex impedance spectroscopic studies of pure and cadmium mixed cobalt levo tartrate crystals were carried out by Manani et al [37] In the present report, the dielectric measurements were done within the frequency range of applied field 10 Hz to 10 MHz and range of temperature from 30°C to 90°C at a step of 20°C. The temperature range is selected below 90°C because magnesium tartrate finds the majority of applications in pharmaceutical formulations, as already mentioned in the introduction part, and hence the low-temperature variations are studied by looking at the physiological temperature limitations.

Figure 5 exhibits the graphical relation between dielectric constant and frequency at various temperatures. Figure 5 reveals that the dielectric constant is higher in the lower frequency region and the dielectric constant decreases as the frequency increases and ultimately becomes almost constant. This is due to the inability of rotating electric dipoles to match with the variation taking place in the applied A.C. electric field. It is also marked that the dielectric constant value decreases slightly as temperature increases within the frequency range under study. The reason for the slight decrease in dielectric constant values on increasing temperature is explained as follows.

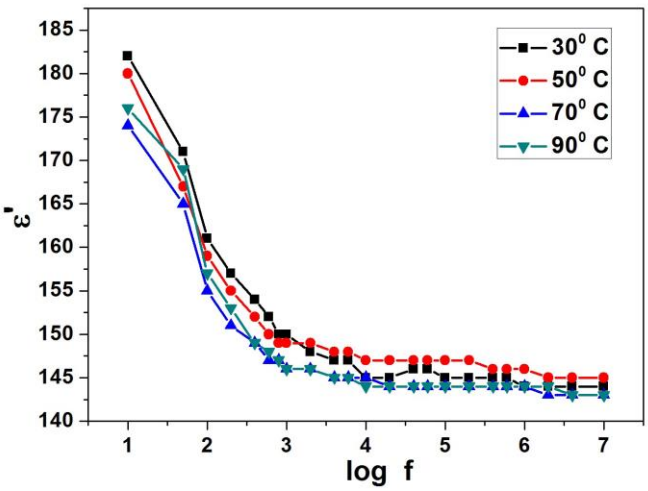

Figure 5. Plot of ε` vs. log f for Magnesium Tartrate nanoparticles

As the temperature increases the kinetic energy increases for the constituent atoms of dipoles and the vibrations in the dipoles also increase and get less tendency to align with the external field. However, for strontium tartrate, the dielectric constant was found to be decreasing within 42°C to 75° C temperature range due to the compensation taking place by the thermal energy leading to the polarization relaxation and dielectric constant resulting from ion-dipole interactions. Thereafter, the dielectric constant was found to increase [30].

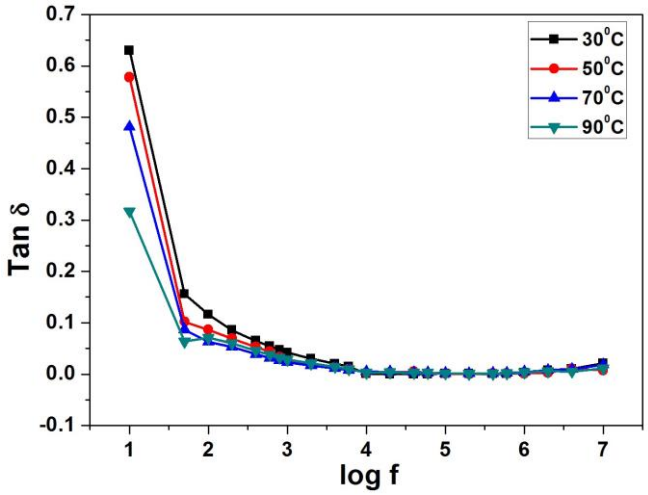

Figure 6. Plot of dielectric loss (δ) vs. log f for Magnesium Tartrate nanoparticles

Figure 6 shows the relation between dielectric loss (tanδ) and log f at various temperatures. The value of dielectric loss (tanδ) decreases as frequency increases. Also, the tan δ decreases as the temperature are raised from room temperature to 90^0C. In the nano-phase materials, the inhomogeneities at the interface layers are likely to produce an absorption current giving dielectric loss-tan δ, which decreases as the frequency of the applied field is increased and hence the resulting dielectric loss reduces [29]. As the temperature increases the dislocation and other defects may coalesce and reduce their number giving rise to the reduced dielectric loss occurring due to defects [38],[39].

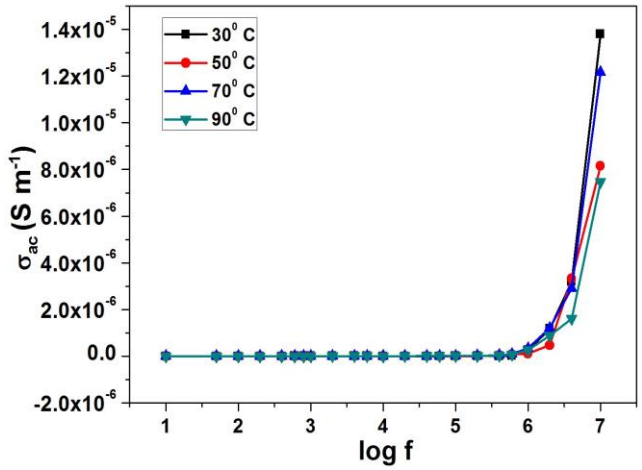

Figure 7. Plot of A.C. conductivity vs. log f for Magnesium Tartrate nanoparticles

Figure 7 is the plot of the A.C. conductivity (σ_{ac}) versus log f for magnesium tartrate nanoparticles. The change in ac conductivity against frequency is due to free or bound charge carriers. In the case of contribution from free charge carriers, the conductivity is decreased with an increase in frequency [40]. As shown in figure 7, the A.C. conductivity increases with increasing frequency for all the temperatures and hence it is due to the contribution of bound charge carriers present in the sample.

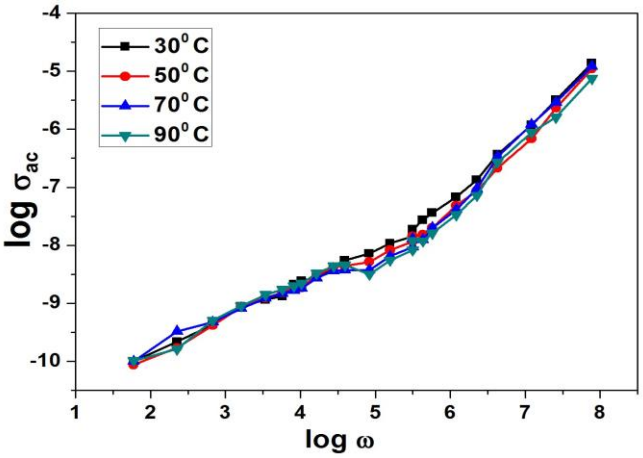

Figure 8 Jonscher's plot

Jonscher's power law is applied to A.C. conductivity data. The Jonscher's power law equation [41], [42] is represented as:

$$\sigma_{ac}(\omega, T) = \sigma_{dc}(T) + A(T)\,\omega^{n} \quad \text{----------(2)}$$

Where σ_{dc} (T) is the D.C. conductivity, the term $a(T)\,\omega^n$ is responsible for the A.C. conductivity because of the dispersion phenomena, A(T) is a constant that depends on temperature and n represents the power-law exponent. Figure 8 shows plots of log σ_{ac} versus log ω, which shows the dispersive nature. However, no major effect of temperature is found within the temperature range studied. The parameters in Jonscher's power law are estimated from the plots of figure 8, which are given in table 3 within the temperature range studied. The variation of exponent *n* along with temperature can predict the mechanism prevailing for A.C. conduction. From table 3, one can predict that Correlated Barrier Hopping (CBH) model is applicable to charge carriers [29]. The parameter A indicates the strength of polarizability and its variation with temperature.

Table 3: The values of parameters *n* and A

Temperature (°C)	*n*	A (S m^{-1} rad^{-n})
30	0.79	1.621×10^{-12}
50	0.75	1.905×10^{-12}
70	0.76	1.862×10^{-12}
90	0.72	2.511×10^{-12}

To study the dependence of A.C. conductivity on frequency and temperature, the Arrhenius plots are drawn at different frequencies using the Arrhenius equation [43].

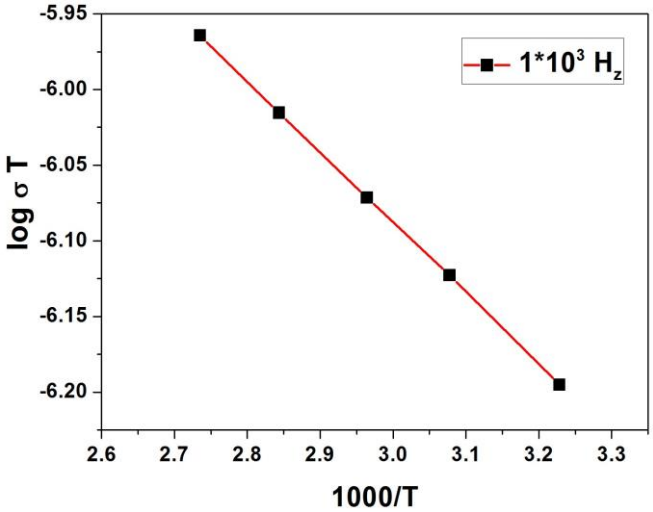

Figure 9. Plot of log (σT) vs. [1000/T] at 1×10^3 Hz

Figure 9 shows the plots drawn for log (σT) vs. [1000/T] at 1 kHz**.** The activation energy for the A.C. conduction is evaluated from the slope of the plot drawn in figure 9. At different frequencies as given in table 4. The activation energy is a potential barrier to be surmounted for in the conduction. Table 4 suggests that the activation energy decreases as the frequency is increased. This further indicates that the A.C. conduction is a kinetic process and as frequency increases, more charge carriers are jumping between the localized states.

Table 4: Activation Energy at Various Temperatures for Magnesium Tartrate Nano Particles

Frequency in Hz	**The activation energy in eV**
1×10^3Hz	0.076eV
1×10^4 Hz	0.059 eV
1×10^5 Hz	0.051eV
1×10^6Hz	0.035 eV
1×10^7Hz	0.018 eV

As mentioned earlier, according to the present authors' knowledge no significant work is reported on magnesium tartrate nano- particles. The nanostructures are expected to give benefits in terms of an increase in the rate of absorption, reduction in the required dose, etc in pharmaceutical applications [44],[45]. The present study on magnesium

tartrate nanoparticles may be helpful to design the needed pharmaceutical formulations.

4. Conclusion

The nano-particles of magnesium tartrate were obtained by wet chemical surfactant mediated technique. The Powder XRD study confirmed orthorhombic crystal structure with cell dimensions a = 9.19Å, b = 11.18 Å, c = 7.96 Å and $\alpha = \beta = \gamma = 90^o$ having the average crystallite size of 40.35 nm and 10.90 nm evaluated by applying Scherrer's formula and Williamson and Hall method, respectively. The TEM images confirmed the nano-structured nature with a size range from 18.25 nm to 48.70 nm and displayed spherical type morphology. FTIR spectrum confirmed the presence of O–H, C–H, C=O functional groups and metal-oxygen vibrations. In comparison to the bulk sample, the redshift and blue shifts occurring in the FTIR spectrum were found as a result of the nano-structured nature. From TGA it was found that the sample remained thermally up to 213°C. During heating in TGA, initially, the sample is converted into an anhydrous form and then into metal oxide via the carbonate stage. DTA shows minor endothermic reactions observed at 60°C temperature is a result of giving up the water of hydration or moisture. The presence of one water molecule was estimated from the calculation. Dielectric constant and dielectric loss both decreased in the same manner as the frequency of applied field was increased at different temperatures. On the application of Jonscher's power law to A.C. conductivity, from the nature of the variation of exponent n along with temperature, the CBH model was found to be applicable for A.C. conduction. From the Arrhenius plots, the A.C. conduction was found to be a thermally activated kinetic process. For future work the author tries to utilize this sample for different biological study as well as to explore paramagnetic iron tartrate nano particles for targeted drug delivery applications.

Acknowledgements
The authors acknowledge the University Grants Commission, New Delhi, for financial assistance under DRS-SAP (III) and the Department of Science and Technology for the FIST. The authors also acknowledge the encouragement from Prof. H. H. Joshi, former Head, Department of Physics, Saurashtra University, Rajkot, and authorities of VIT University, Vellore, for the experimental facility. The author (PMV) is thankful to the Principal, Kamani Science College, Amreli for their support.

Conflict of Interest
This copy has not been communicated or is in process anywhere else. Therefore, there is no conflict of the addicted for us to encounter.

Data Availability
The raw data required to ongoing study; hence it cannot be shared.

Funding Resources
There was no external funding for this study.

Authors contribution
The first author U. M. Lathiya has synthesized samples and analysed the structural properties of samples and wrote the first draft of the manuscript. Other authors M.J.Joshi and P.M.Vyas helped her during the synthesis and writing of the papers effectively.

References

[1] H. K. Henisch, J. Dennis, J. I. Hanoka, "Crystal growth in gels", *Journal of Physics and Chemistry of Solids*, Vol. **26**, Issue **3,** pp. **493-496**, **1965 .** https://doi.org/10.1016/0022-3697(65)90123-X

[2] P. M. Vyas, H. O. Jethva, S. J. Joshi, M. J. Joshi, "The roles of gel medium and gelling solution in the growth of the crystals: A case study of calcium levo-tartrate", *Archives of Physics Research,* Vol. **4**, Issue **6,** pp. **9-15**, **2013**

[3] U. V. Tarpara, P. M. Vyas, M. J. Joshi, "Synthesis and characterization of calcium tartrate dehydrate nanoparticles", *International Journal of Nanoscience*, Vol.**14**, Issue**3,** pp.**1550013(1)-1550013(6)**, **2015.** https://doi.org/10.1142/S0219581X15500131

[4] S. J. Joshi, K. P. Tank, P. M. Vyas, M. J. Joshi, "Structural, FTIR, thermal and dielectric studies of gel grown manganese–copper mixed levo tartrate crystals", *Journal Crystal Growth*, Vol. **401**, pp. **210-214**, **2014** Doi.10.1016/ j. crysgro.2014.01.060

[5] H. O. Jethva, P. M. Vyas, K. P. Tank, M. J. Joshi, "FTIR and thermal studies of gel-grown, lead–cadmium-mixed levo tartrate crystals", *Journal of Thermal Analysis and Calorimetry*, Vol. **117**, pp. **589-594 2014** Doi.10.1007/s 10973-014-3770-1

[6] R. M. Dabhi, B. B. Parekh, M. J. Joshi, "Dielectric studies of gel grown zinc tartrate crystals", *Indian Journal of Physics*, Vol. **79**, Issue **5,** pp. **503-507**, **2005**

[7] V. S. Joshi, M. J. Joshi, "FTIR spectroscopic and thermal studies of calcium tartrate trihydrate crystals grown by gel assistance", *Indian Journal of Physics*. **75A**, Issue **2** pp. **159-163**, **2001**

[8] S. Joseph, H. S. Joshi, M. J. Joshi, "Infrared spectroscopic and thermal studies of gel grown spherulitic crystals of iron tartrate", *Crystal Research & Technology*, Vol. **32**, Issue **2,** pp. **339-346**, **1997**

[9] U. M. Lathiya, H. O. Jethva, P. M. Vyas, M. J. Joshi, "Powder XRD, TEM, FTIR and thermal studies of strontium tartrate nano particles", *Functional Oxides and Nanomaterials,* American Institute of Physics, *AIP Conf Proceed* **1837**, pp. **040015(1)-040015(3) 2017** Doi.10.1063/1:4982099

[10] K. C. Kam, K. L. M. Young, A. K. Cheetham, "Chemical and Structural Diversity in Chiral Magnesium Tartrates and their Racemic and Meso Analogues", *Crystal Growth & Design*, Vol. **7**, Issue **8**, pp. **1522-1532**, **2007** DOI**:** 10.1021/cg070388a

[11] K. K. Ghara, P. Maiti, P. K. Ghosh, "Correlation of Filtration Behavior of Chiral and Racemic Mg(tartrate) Suspensions with Morphological Differences and Observation of Cross Structure in a Metal Organic Framework", *Industrial & Engineering Chemistry Research*,Vol. **54**, Issue **13,** pp. **3320-3325, 2015** DOI**:** 10.1021/ie5047973

[12] L. S. Jacob, T. J. Williams, R. D. Krell, "Non-aqueous colonic purgative formulations", *Patent,* **EP0934071 A4** oct. 8, **1998**

[13] L. W. Coleman, "Laser Program Overview, Laser program Annual Report", *Lawerence Livermose National Lab*, UCRL – **50021 – 87**, **1987**

[14] M. S. Mastuli, N. S. Ansari, M. A. Nawawi, A. M. Mahat, "Effects of cationic surfactant in sol-gel synthesis of nano sized magnesium oxide", Elsevier B.V. Selection and/or peer review under responsibility of Asia-Pacific Chemical, Biological & Environmental Engineering Society ,*APCBEE Procedia*, Vol. **3**, pp. **93-98**, **2012** https://doi.org/10.1016/j.apcbee.2012.06.052

[15] R. Jaffe, "Enhancement of magnesium uptake in mammals", *US Patent*, **8017160B2**, sep. 13,**2011**

[16] P. C. Hllson, G. A. Rose, In P. O. Schwille, L. H. Smith, W. G. Robertson, W. Vahlensieck, "The additive effects of magnesium and tartrate upon inhibition of calcium oxalate crystal formation in whole urine", eds, Urolithiasisand Related Research, Springer , Boston, USA, Vol. **62**, Issue **1** pp. **17-19**, **1982**

[17] Z. Hui, C. Cui – Yuan, O. Jian – Ming, "Modulation of Magnesium Tartrate on Crystal Growth of Hydrate Calcium Oxalates", *Chemical Journal of Chinese Universities -Chinese Edition*, Vol. **27**, Issue **7**, pp. **1220-1222**, **2006**

[18] M. P. Dave, S. A. Gandhi, V. Joshi, "Powder XRD and FTIR Study of Magnesium Levo-Tartrate", *International Journal of Innovative Research in Science, Engineering and Technology*, Vol. **5**, Issue **1**, pp. **1020-1026, 2016**

[19] K. K. Ghara, N. Korat, D. Bhalodiya, J. Solanki, P. Maiti, P. K. Ghosh, "Production of pure potassium salts directly from sea bittern employing tartaric acid as a benign and recyclable K^+ precipitant", *RSC Advances*, Vol. **4**, Issue **65**, pp. **34706-34711, 2014**, DOI**:**10.1039/C4RA04360J

[20] P. Solanki, S. Vasant, M. Joshi, "Synthesis, crystal structure, spectroscopic and thermal analysis of strontium pyrophosphate dihydrate nanoparticles", *International Journal of Applied Ceramic Technology*, Vol.**11,** Issue.**4,** pp.**663-669**, **2014** https://doi.org/10.1111/ijac.12227

[21] T. P. Yendrapati, V. R. Kalagadda, S. S. Vemula, S. Bandla, "X-Ray Analysis by Williamson-Hall and Size-Strain Plot Methods of ZnO Nanoparticles with Fuel Variation", *World Journal of Nano Science and Engineering*, Vol. **4**, Isuue **1**, pp. **21-28**, **2014,** DOI:10.4236/wjnse.2014.41004

[22] S. Kurien, "Structural and Electrical Properties of Certain Nanocryatalline Aluminates", Ph. D. Thesis, Dept. of St. Berchmans College, Mahatma Gandhi University, Kerala **2005**

[23] K. P. Tank, "Synthesis characterization and inhibition study of pure and doped nano-apatites", Ph. D. Thesis, Dept. of physics, Saurashtra University, Rajkot, Gujrat, **2013**

[24] N. Colthup, L. Daly, S. Wiberly, "Introduction to Infrared and Raman Spectroscopy" 3rd Edition, Elsevier Publisher, Academic Press **1990,** ISBN: 9780080917405

[25] C. B. Mohmed, K. Karoui, S. Saidi, K. Guidara, A. B. Rhaiem, "Electrical properties, phase transitions and conduction mechanisms of the $[(C_2H_5)NH_3]_2CdCl_4$ compound", *Physica B*, Vol.**451**, pp.**87-95**, **2014** DOI:http://dx.doi.org/10.1016/j.physb.2014.06.006.

[26] M. A. Fakhree, D. R. Delgado, F. Martinez, A. Jouyban, "The Importance of dielectric Constant for drug solubility prediction in binary solvent mixtures: electrolytes and zwitterions in water+ethanol", *AAPS Pharm. Sci. Tech*., Vol. **11**, Issue **4**, pp. **1726-1729**, **2010** DOI: 10.1208/s12249-010-9552-3

[27] J. F. Riordan, "The role of metals in enzyme activity", *Annals of clinical and Laboratory Science*, Vol. **7**, Issue **2**, pp. **119-129**, **1977**

[28] E. L. Mertz, L. I. Kristalik, "Low dielectric response in enzyme active site", *Proceedings of the National Academy of Sciences*, USA. Vol. **97**, Issue **5**, pp. **2081-2086**, **2000** https://doi.org/10.1073/pnas.050316997

[29] S. R. Vasant, "Synthesis and characterization of pure and doped calcium pyrophosphate nano-particles", Ph. D. Thesis, Dept. of physics, Saurashtra University, Rajkot, Gujrat, **2015**

[30] S. K. Arora, V. Patel, B. Amin, A. Kothari, "Dielectric behaviuor of strontium tartrate single crystals", *Bulletin of Materials Science*, Vol. **27**, Issue **2,** pp. **141-147**, **2004** DOI:10.1007/BF02708496

[31] S. K. Arora,T. Mathew, "Dielectric studies of $CuWO_4$ crystals", *Physica Status Solidi A*, Vol. **116**, Issue **1**, pp. **405-413 1989** https://doi.org/10.1002/pssa.2211160141

[32] G. K. Solanki, D. B. Patel, K. D. Patel, N. N. Gosai, Y. G. Mansur, "Growth and dielectric properties of DVT grown $GeS_{0.25}Se_{0.75}$ single crystals", *Physical Chemistry*., Vol. **2**, Issue **5**, pp. **67-72, 2012** DOI: 10.5923/j.pc.20120205.02

[33] M. D. Shah, B. Want, "Growth, characterization and dielectric studies of gadolinium fumarate heptahydrate single crystals", *Bulletin of Material Sci*ence, Vol. **38**, Issue **1**, pp. **73-81**, **2015**

[34] J. H. Joshi, D. K. Kanchan, H. O. Jethva, M. J. Joshi, K. D. Parikh, "Dielectric relaxation, protonic defect, conductivity mechanisms, complex impedance and modulus spectroscopic studies of pure and L-threonine-doped ammonium dihydrogen phosphate", *Ionics*, Vol. **24,** Issue **2**, pp. **1995-2016**, **2018** Doi.10.1007/511581-018,2461-2

[35] Z. Imran, M. A. Rafiq, M. Ahmad, K. Rasool, S. S. Batool, M. M. Hasan, "Temperature dependent transport and dielectric properties of cadmium titanate nanofiber mats", *AIP Advances*, Vol. **3**, pp .**032146(1)-032146(13)**, **2013** https://doi.org/10.1063/1.4799756

[36] B. D. Shrivastav, R. Barde, A. Mishra, S. Phadake, "Frequency and Temperature Dependence of Dielectric Properties of Fish Scales Tissues", *Research Journal of Physical Sci*ence, Vol. **1,** Issue **6**, pp. **24-29**, **2013**

[37] N. H. Manani, H. O. Jethva, M. J. Joshi "Dielectric Relaxation, Conductivity Mechanism and Complex Impedance Spectroscopic Studies of Pure and Cadmium Mixed Cobalt Levo-Tartrate Crystals", *International Journal of Scientific Research in Physics and Applied Sciences*, Vol. **8**, Isuue **1**, pp. **8-15**, **2020** DOI:10.26438/ijsrpas/v8i1.815

[38] A. I. Osetskii, "Low-temperature fluctuational motion of dislocations in crystals I. Quantum and dissipative effects", *Physica Status Solid: B*, Vol. **117**, Issue **1**, pp. **355-365**, 1983. https://doi.org/10.1002/pssb.2221170140

[39] J. Friedel, "Dislocation: International Series of Monographs on Solid State Physics", *first edition*, Elsevier Publisher, **1964** ISBN: 9781483135922

[40] M. N. Kamalasanan, N. D. Kumar, S. Chandra, "Dielectric and ferroelectric properties of $BaTiO_3$ thin films grown by the sol-gel process", *Journal of Applied Phys*ics, Vol. **74,** Issue **9,** pp. **5679-5686**, **1993** https://doi.org/10.1063/1.354183

[41] A. K. Jonscher, "The universal dielectric response", *Nature*, Vol. **267,** pp. **673-679**, **1977,** DOI:10.1038/267673a0

[42] J. O. L`opez, R. G. Aguilar, "Dielectric permittivity and AC conductivity in polycrystalline and amorphous C_{60}", *Revista Mexicana de Fis*ica, Vol. **49**, Issue **6**, pp. **529-536**, **2003**.

[43] H. Mahamoud, B. Louati, F. Hlel, K. Guidara, "Conductivity and dielectric studies on $(Na_{0.4}Ag_{0.6})_2PbP_2O_7$ compound", *Bulletin of Material Science*, Vol. **34**, Issue **5**, pp. **1069-1075**, **2011**

[44] M. J. Joshi, "Opportunities, challenges and pathways of nano-medicines: a concise review", *Journal of Nanomedicine Res*earch, Vol. **1**, Issue **2**, pp. **63-64**, **2014**, DOI: 10.15406/jnmr.2014.01.00013

[45] M. J. Joshi, "Interdisciplinary approach to nano – crystalline active pharmaceutical ingredients: a brief review", *International Journal of ChemTech Research*., Vol. **6**, Issue **3**, pp. **1800-1802**, **2014**

AUTHORS PROFILE

Dr. U. M. Lathiya earned his B. sc., M. sc., M. Phil. and Ph.D. in physics from Saurashtra University in 2006, 2008, 2012 and 2020, respectively. She is currently working as assistant Professor in Department of Humanities and Social Science from SSASIT, Surat since 2010. She has published 3 research papers in reputed international journals and conferences. It's also available online. His main research work focuses on Nano materials. She has 13 years of teaching experience.

Prof. Dr. M. J. Joshi is a post graduate from Saurashtra University, Rajkot, Gujarat and Doctorate from the same university. He has published more than one hundred fifty research papers in International Journals of repute and has an experience of teaching Physics to post graduate students for more than thirty one years. He has guided more than twenty students for Doctorate

degree and twenty students for M.Phil. degree. He is active as a subject referee in various journals of International repute. He has refereed more than sixty five Ph.D. Thesis. He has worked as Head and Professor of Physics in the same university. Currently, he is retired.

Lt. Dr. P. M. Vyas is a post graduate from Saurashtra University, Rajkot, Gujarat and Doctorate from the same University. He has published more than twenty seven research papers in International Journals of repute and four books for the undergraduate students of the same University. He holds an experience of teaching Physics to undergraduate students for more than twelve years. Currently he is working as an Asst. Professor at Kamani Science College and Prataprai Arts College, Amreli, Gujarat and also working as a company commander of National Cadet Corps in the same college.

